Virologica Sinica (2021) 36:667–677
https://doi.org/10.1007/s12250-020-00342-y

www.virosin.org
www.springer.com/12250

RESEARCH ARTICLE

Axl Alleviates Neuroinflammation and Delays Japanese Encephalitis Progression in Mice

Zhao-Yang Wang[1] · Zi-Da Zhen[1] · Dong-Ying Fan[1] · Pei-Gang Wang[1] · Jing An[1,2]

Received: 6 July 2020 / Accepted: 7 December 2020 / Published online: 3 February 2021

Abstract

Japanese encephalitis virus (JEV) is a mosquito-borne flavivirus, which causes the most commonly diagnosed viral encephalitis named Japanese encephalitis (JE) in the world with an unclear pathogenesis. Axl, a receptor tyrosine kinase from TAM family, plays crucial role in many inflammatory diseases. We have previously discovered that Axl deficiency resulted in more severe body weight loss in mice during JEV infection, which we speculate is due to the anti-inflammatory effect of Axl during JE. Currently, the role of Axl in regulating the neuroinflammation and brain damage during JE has not been investigated yet. In this study, by using Axl deficient and heterozygous control mice, we discovered that Axl deficient mice displayed accelerated JE progression and exacerbated brain damage characterized by increased neural cell death, extended infiltration of inflammatory cells, and enhanced production of pro-inflammatory cytokines, in comparison to control mice. Additionally, consistent with our previous report, Axl deficiency had no impact on the infection and target cell tropism of JEV in brain. Taken together, our results suggest that Axl plays an anti-inflammatory and neuroprotective role during the pathogenesis of JE.

Keywords Axl · Japanese encephalitis virus (JEV) · Inflammation · Cytokine

Introduction

Japanese encephalitis virus (JEV), like dengue virus (DENV), Zika virus (ZIKV), and West Nile virus (WNV), belongs to the genus *Flavivirus* and family *Flaviviridae* and is the pathogenic agent of Japanese encephalitis (JE), which mainly prevails in Asia and Southeast Asia, renders more than two billion people at risk, and thus is the most important viral encephalitis in the world (Turtle and Solomon 2018). Unlike DENV or ZIKV, JEV is much more neuroinvasive, and JEV invasion into brain usually results in severe encephalitis. The average fatality rate of JE is 20%, in children the fatality can be 30% (Amicizia *et al.* 2018). About 50% of JE patients develop permanent neurological sequelae. Despite the great disease burden of JE, we currently know little about JE pathogenesis and have no specific therapy for it (Turtle and Solomon 2018).

Axl, a key member of receptor tyrosine kinase TAM family (the other two members are Tyro3 and Mertk), plays a key role in immune and inflammatory homeostasis (Rothlin *et al.* 2007). Axl is universally expressed in multitudinous cells, such as macrophages and dendritic cells (Rothlin *et al.* 2015). Gas6 broadly existing in the humoral fluid is the natural ligand for Axl. Cells utilize Axl to identify and bind to phosphatidylserines on the surface of apoptotic cells via bridging by Gas6, which promotes the phagocytic clearance of apoptotic cells and averts inflammatory response (Seitz *et al.* 2007). Ligation of Axl to phosphatidylserines also activates Axl signaling pathway and promotes the expression of suppressor of cytokine signaling (SOCS) 1 and SOCS3, which suppress the production of many pro-inflammatory cytokines such as TNF-α, IL-1β, and IL-6 (Rothlin *et al.* 2007; Sun *et al.* 2010). Interestingly, many enveloped viruses also hold phosphatidylserines on their surface, these phosphatidylserines can bind to Axl expressed on surface of

Zhao-Yang Wang and Zi-Da Zhen have contributed equally to this work.

✉ Pei-Gang Wang
pgwang@ccmu.edu.cn

[1] Department of Microbiology, School of Basic Medical Sciences, Capital Medical University, Beijing 100069, China

[2] Center of Epilepsy, Beijing Institute for Brain Disorders, Beijing 100093, China

host cells and facilitate virus entry (Moller-Tank and Maury 2014). Flaviviruses including DENV, ZIKV, and WNV can exploit Axl to promote entry (Richard *et al.* 2017). However, the roles of Axl in flavivirus infection are far beyond a receptor. During ZIKV infection, besides acting as an entry receptor, Axl also attenuates the production of type I interferon and inflammatory cytokines to favor viral replication (Meertens *et al.* 2017; Chen *et al.* 2018; Strange *et al.* 2019).

The roles of Axl in encephalitis have been less studied. Activation of Axl signaling attenuates neuroinflammation and reduces neurological deficits after ischemic stroke (Wu *et al.* 2018). Loss of Axl signaling causes extensive axonal damage, prolonged neuroinflammation, and less remyelination after cuprizone exposure (Ray *et al.* 2017). Weinger *et al.* found that $Axl^{-/-}$ mice manifest more spinal cord lesions with larger inflammatory cuffs, more demyelination, and more axonal damage than wild type mice during experimental autoimmune encephalomyelitis (Weinger *et al.* 2011). These findings suggest that Axl plays an anti-inflammatory and neuroprotective role during various kinds of encephalitis. We have previously reported that during JEV infection, Axl deficient mice displayed significantly more body weight loss than control mice, which we speculate it is the result of the anti-inflammatory role of Axl. Notwithstanding, there is no research discussing the role of Axl in regulating viral encephalitis, let alone Japanese encephalitis. Whether Axl negatively regulates inflammatory response in brain during JEV infection remains unknown.

In this research, by using Axl deficient mice and littermate heterozygous control, we discovered that Axl deficiency accelerated JE progression, which was correlated with exacerbated brain lesions induced by JEV, including increased neuron death, enhanced inflammatory cytokines production, and extended cytotoxic immune cells infiltration. These results suggest that Axl may be an anti-inflammatory factor during JEV infection, which provides a potential target for alleviating inflammatory damage of JE.

Materials and Methods

Cells and Virus

C6/36 cells were grown in RPMI 1640 medium (Gibco, USA) supplemented with 10% fetal bovine serum (FBS, PAN, Germany) and maintained at 28 °C. Vero cells were grown in minimum essential medium (MEM, Gibco, USA) supplemented with 5% FBS and maintained at 37 °C. JEV Beijing strain-1 (JEV) (Sheng *et al.* 2016) was propagated in C6/36 cells and titrated on Vero cells by plaque assay as previously reported (Wang *et al.* 2018).

Mice

Axl deficient ($Axl^{-/-}$) mice were kind courtesy of Dr. Dai-Shu Han (Peking Union Medical College, Beijing, China) and originally developed by Dr. Greg Lemke (Salk Institute for Biological Studies, La Jolla, CA). Mice were raised under a specific pathogen-free animal facility at Capital Medical University, China. The F_0 $Axl^{-/-}$ mice were generated from C57BL/6 J mice and were mated with F_0 wild type ($Axl^{+/+}$) C57BL/6 J mice to generate F_1 heterozygous ($Axl^{+/-}$) mice. The F_0 $Axl^{-/-}$ mice were then mated with F_1 $Axl^{+/-}$ mice to generate F_2 $Axl^{-/-}$ mice (experimental group) and littermate F_2 $Axl^{+/-}$ mice (control group). The littermate $Axl^{+/-}$ mice are ideal controls for $Axl^{-/-}$ mice due to same age, similar nutritional and living status, and close genetic background. The genotype of F_2 mice were identified by PCR, and three primers were used: Wt: 5′-GCCGAGGTATAGTCTGTCACAG-3′; Mut: 5′-TTTGCCAAGTTCTAATTCCATC-3′; WtMut: 5′-AGAAGGGGTTAGATGAGGAC-3′. The sizes of PCR products are 350 bp for $Axl^{+/+}$ mice, 350 and 200 bp for $Axl^{+/-}$ mice, and 200 bp for $Axl^{-/-}$ mice.

Animal Infection

Four-week-old $Axl^{+/-}$ and $Axl^{-/-}$ mice were intraperitoneally (i.p.) injected with 10^4, 10^5, and 10^6 PFU of JEV in 200 μL of phosphate buffered saline (PBS), or just 200 μL of PBS in mock-treated mice.

Hematoxylin and Eosin (HE) Staining

Brains of $Axl^{+/-}$ and $Axl^{-/-}$ mice were collected at 7 days post infection (dpi). The brains were immersed in 4% paraformaldehyde (PFA in PBS) for 24 h, then stored in 75% ethanol for paraffin embedding and section. Paraffin embedded brains were sagittally sectioned into 5 μm slides, which were then subjected to standard H&E staining procedures. The statistical analysis of HE staining results was completed by using Image-pro Plus 6.0 and GraphPad Prism 7.00 software.

Immunofluorescent (IF), Immunohistochemical (IHC), and TUNEL Staining

Brains of $Axl^{+/-}$ and $Axl^{-/-}$ mice were harvested at 7 dpi. The left brains were embedded in OCT (4583, SAKURA) for cryosection. The right brains were immersed in 4% PFA for paraffin embedding and section. OCT embedded brains were sagittally cryo-sectioned into 6 μm slides and were fixed with ice cold acetone. Paraffin embedded brains

were sectioned into 5 μm slides. For IF staining, after membrane permeability with 0.5% Triton and blockage with 1% bovine serum albumin (BSA), the brain sections were incubated with anti-JEV mouse serum (self-made) and anti-NeuN (ab104224, Abcam), anti-GFAP (ab7260, Abcam), or anti-Iba1 (10,904–1-AP, Proteintech) in 1:300 dilution at 4 °C overnight and followed by incubation with Alexa Fluor 488 labeled donkey anti-mouse IgG antibody (A21202, Thermo) and Alexa Fluor 594 labeled donkey anti-rabbit IgG antibody (A21207, Thermo) in 1:500 dilution at room temperature for 40 min. For IHC staining, a heat mediated antigen retrieval was performed prior to primary antibody incubation with anti-CD4 antibody (ab183685, Abcam), anti-CD8 antibody (98941S, CST), and anti-SMI32 (SMI-32P, BioLegend), then an IHC kit (SNP-9001, Histostain) were used to visualize CD4, CD8, and SMI32 in brain tissues. For TUNEL staining, One Step TUNEL Apoptosis Assay Kit (C1086, Beyotime) was used according to the manufacture's instruction.

Flow Cytometry

The mice were anesthetized and perfused with 60 mL of PBS at 7 days post infection. Brain tissue was isolated and the cerebral cortex and hippocampus were separated and immersed in digestive solution (0.25% trypsin and 0.02% EDTA in PBS) at 37 °C for 25 min with gentle shake followed by termination with equal volume of 10% FBS DMEM. After standing for 2 min, the supernatant was aspirated and filtered with 200 mesh filter followed by centrifugation at 1200 $\times g$ for 5 min. The cell pellet was resuspended with PBS and fixed with 32% paraformaldehyde to a final concentration of 4% at 37 °C for 10 min, followed by membrane permeability with 90% methanol on ice for 10 min. The cells were then blocked with 1% BSA at 37 °C for 10 min, followed by incubation with CD4 (553,046, BD) and CD8 antibody (560,182, BD) at room temperature for 1 h. The cells were then resuspended in PBS and subjected to flow cytometry by using Cytoflex system (Beckman).

Multiplex Immunoassay

Brains of $Axl^{+/-}$ and $Axl^{-/-}$ mice i.p. injected with 10^4 PFU of JEV were collected at 7 dpi and homogenized in 1 × cell lysis buffer (9803S, CST), followed by centrifugation at 12,000 $\times g$ for 10 min to collect supernatants. Resulting supernatants were subjected to a bead-based immunoassay (Aimplex) to measure the contents of a panel of cytokines (IL-1α, IL-1β, IL-2, IL-4, IL-6, IL-10, TNF-α, IFN-γ, CCL2, and CCL5).

Statistical Analysis

The quantitative data were expressed as the mean ± SEM and all the statistical analyses were performed on GraphPad Prism 7.00 software. Student's t test or with Welch's correction and Mann–Whitney test were used to compare data between two groups. Difference was considered to be statistically significant when $P < 0.05$.

Results

Axl Deficiency Accelerates the Progression of Japanese Encephalitis (JE)

$Axl^{-/-}$ and $Axl^{+/-}$ (control) mice were i.p. injected with diverse dose of JEV (10^4, 10^5 and 10^6 PFU per mouse). Similar to the infection pattern in humans, in our mouse model, there were only two outcomes of JEV infection, namely inapparent and apparent infection (Fig. 1). Mice with inapparent infection showed no signs or loss of body weight, while mice with apparent infection manifested typical signs of JE and eventually died. About 6–7 days post infection (dpi), a fraction of mice, which positively correlated with infection dose, commenced to lose body weight and became sluggish (onset of encephalitis). As the disease progressed, these mice manifested ruffled fur, hunched back, limb paralysis successively, and finally died (Fig. 1). The time span from viral inoculation to the first observation of body weight loss was defined as the incubation period, and the time span from the first observation of body weight loss to death was defined as the disease duration. As expected, with the increase of infection dose, the incubation period was gradually shortened, but at all infection doses, the incubation period in $Axl^{-/-}$ and control mice was similar (Fig. 2A–2C). However, $Axl^{-/-}$ mice displayed shorter time of disease duration than $Axl^{+/-}$ mice (Fig. 2D–2F). These results suggest that Axl deficiency may accelerate disease progression in mice with apparent JE.

Axl Deficiency Exacerbates JE-Induced Brain Damage

To test whether Axl deficiency accelerates JE progression by facilitating viral infection and/or exacerbating brain lesions induced by JEV, we examined viral infection and pathological changes in brains at 7 dpi using immunofluorescent (IF) staining and hematoxylin–eosin (HE) staining respectively. JEV antigens mainly distributed in cerebral cortex and hippocampus, and $Axl^{-/-}$ mice showed similar JEV distribution pattern in brain with control mice (Fig. 3).

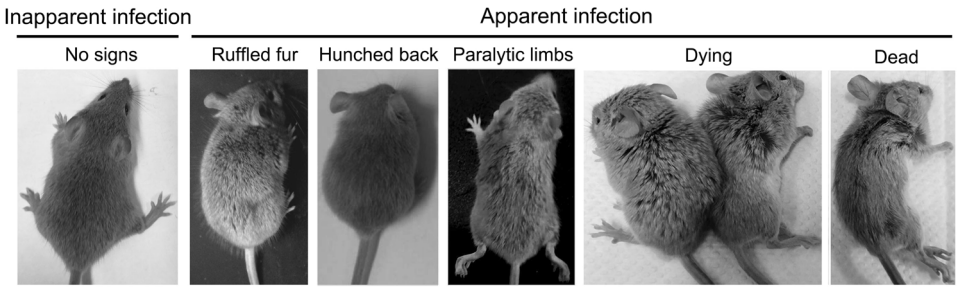

Fig. 1 Signs of Japanese encephalitis virus (JEV) infection. Four-week-old $Axl^{+/-}$ and $Axl^{-/-}$ mice are intraperitoneally (i.p.) injected with 10^4 PFU of JEV. The infection patterns are classified into inapparent infection, where no signs of infection appear, and apparent infection, where the signs vary from ruffled fur, hunched back, paralytic limbs, dying, to death.

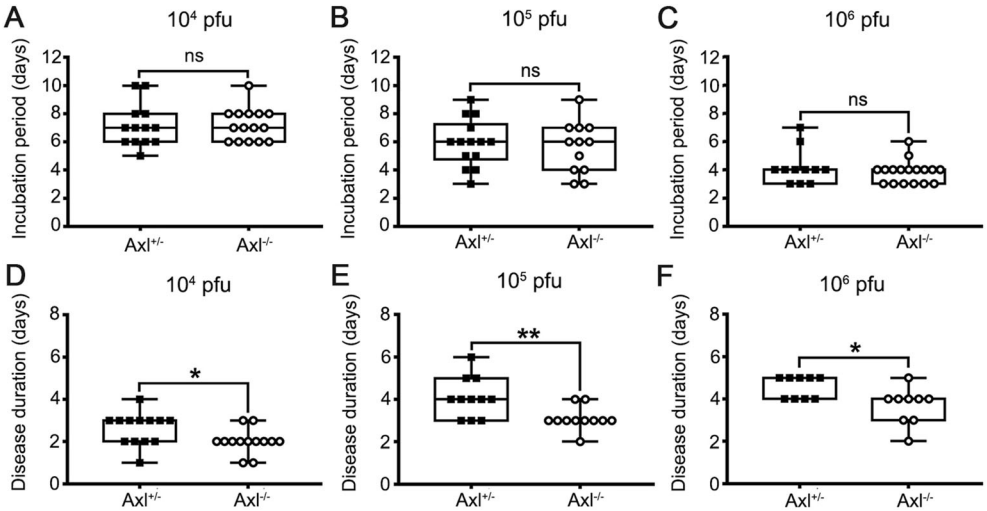

Fig. 2 Incubation period and disease duration of Japanese encephalitis (JE). Four-week-old $Axl^{+/-}$ and $Axl^{-/-}$ mice are intraperitoneally injected with various dose of JEV. **A–C** Incubation period of $Axl^{+/-}$ and $Axl^{-/-}$ mice infected with 10^4 (**A**), 10^5 (**B**), and 10^6 (**C**) PFU of JEV. **D–F** Disease duration of $Axl^{+/-}$ and $Axl^{-/-}$ mice infected with 10^4 (**D**), 10^5 (**E**), and 10^6 (**F**) PFU of JEV. Data are expressed as the median + upper and lower quartiles, and each dot represents a mouse, * $P < 0.05$, as analyzed by Mann–Whitney test.

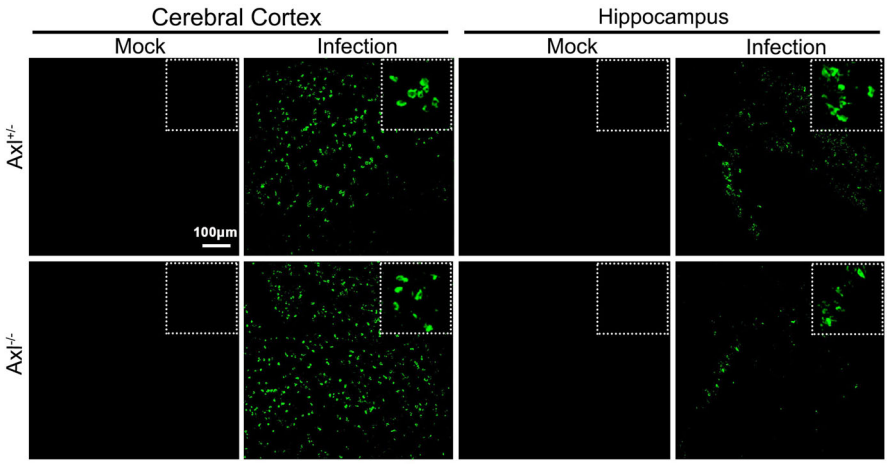

Fig. 3 Distribution pattern of JEV in brain. Four-week-old $Axl^{+/-}$ and $Axl^{-/-}$ mice were intraperitoneally. injected with 10^4 PFU of JEV (infected) or PBS (mock). Brains were harvested at 7 dpi and subjected to IF staining of JEV antigens (green), scale bar = 100 μm.

JEV mainly infected neurons ($NeuN^+$), rather than astrocytes ($GFAP^+$) or microglia ($Iba1^+$) in brain, and $Axl^{-/-}$ mice displayed identical target cell tropism as control mice (Fig. 4). These results suggest that Axl is not an essential factor for JEV infection in brain. On the other hand, in both $Axl^{-/-}$ and control mice, conspicuous lesions in brains were observed, including neural cell loss (mainly in cerebral cortex and hippocampus), infiltration of inflammatory

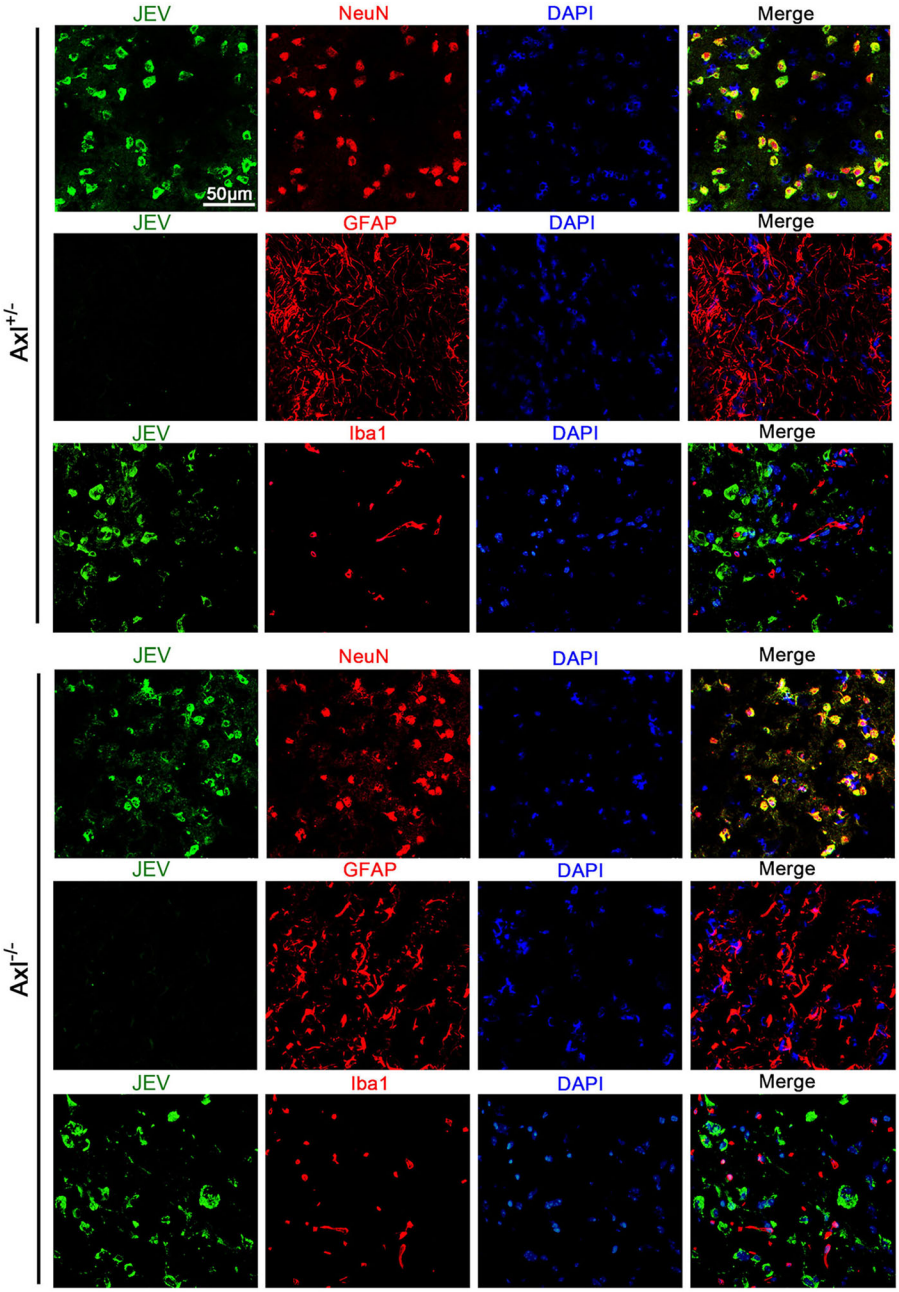

Fig. 4 Immunofluorescent co-staining of JEV antigens and neural cell markers. Four-week-old $Axl^{+/-}$ and $Axl^{-/-}$ mice were intraperitoneally injected with 10^4 PFU of JEV. Brains were collected at 7 dpi and cryo-sectioned into 6 μm slides. JEV antigens (green) were co-stained with NeuN (a marker for neuron, red), GFAP (a marker for astrocyte, red) and Iba1 (a marker for microglia, red) in cerebral cortex. DAPI denotes nucleus, scale bar = 50 μm.

cells, angiectasis (vascular dilation), perivascular cuffing and disorganization of cerebral cortex architecture (Fig. 5A and 5B). Notably, $Axl^{-/-}$ mice showed much more neuron loss in cerebral cortex and hippocampus (Fig. 5A and 5C), more severe angiectasis in deeper cerebral cortex and cerebellum (Fig. 5A, 5B, and 5D), greater area of perivascular inflammatory cells infiltration than control mice (Fig. 5B and 5E). Neurofilaments (NF) are approximately 10 nm intermediate filaments found in neurons. They are a major component of the neuronal cytoskeleton, and function primarily to provide structural support for the axon and to regulate the axon diameter (Yuan *et al.* 2017). We observed the axonal damage by staining neurofilament and found that $Axl^{-/-}$ mice showed significantly reduced and thinned staining of neurofilaments in brain than $Axl^{+/-}$ mice during JE (Fig. 6). These results suggest that Axl deficiency enhances neuroinflammation and brain lesions during JE.

We next study the effect of Axl on the apoptosis of JEV-infected neurons by using immunofluorescent staining of cleaved caspase 3 and TUNEL staining of damaged genome DNA. Although $Axl^{-/-}$ and $Axl^{+/-}$ mice showed similar expression of JEV in brain, $Axl^{-/-}$ mice showed significantly increased expression of cleaved caspase 3

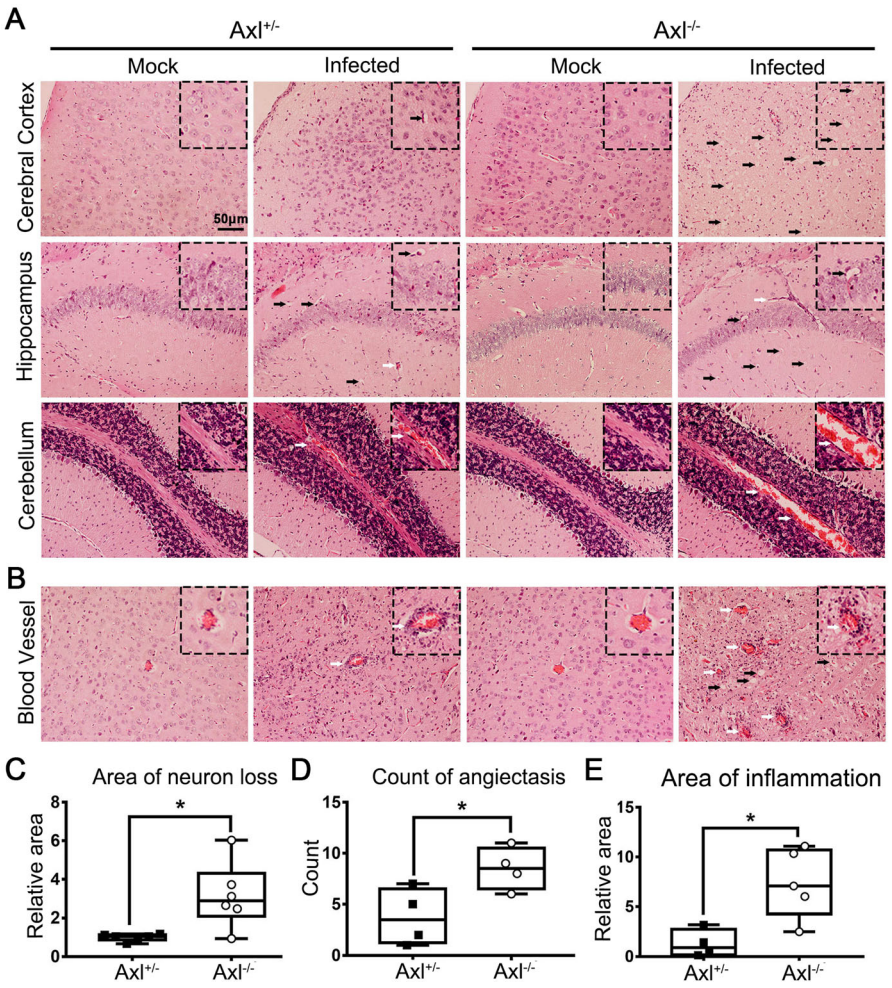

Fig. 5 Pathological damage in brain during JE. Four-week-old $Axl^{+/-}$ and $Axl^{-/-}$ mice were intraperitoneally injected with 10^4 PFU of JEV (infected) or PBS (mock). Brains were collected at 7 dpi and sagittally sectioned into 5 μm slides. **A, B** HE image showing neuron death (black arrow) and angiectasis (white arrow) in brains of JE present mice at 7 dpi, scale bar = 50 μm. **C–E** Quantitative analysis of the area of neuron loss (**C**), count of angiectasis (**D**), and area of inflammatory cell infiltration (**E**). The area data of neuron loss and inflammatory cell infiltration were normalized to the average of JEV-infected $Axl^{+/-}$ mice. Data were expressed as the median + upper and lower quartiles, and each dot represents a mouse, * $P < 0.05$, as analyzed by Mann–Whitney test.

(activated form) in brain (Fig. 7A). The apoptosis of neurons in $Axl^{-/-}$ mice was also more obvious than $Axl^{+/-}$ mice (Fig. 7B). These results suggest that Axl deficiency promotes the apoptosis of JEV-infected neurons.

Axl Deficiency Enhances T Lymphocytes Infiltration in Brain

To further characterize the infiltration of inflammatory cells in brain, we performed immunohistochemical (IHC) staining of $CD8^+$ T cells and $CD4^+$ T cells. In brains of $Axl^{-/-}$ and control mice showing JE at 7 dpi, $CD8^+$ T cells were widely distributed in whole brain, mainly in cerebral cortex, perivascular regions, hippocampus and cerebellum (Fig. 8A). $Axl^{-/-}$ mice showed greater number of $CD8^+$ T cells in cerebral cortex (Fig. 8B), perivascular region (Fig. 8C), hippocampus (Fig. 8D), and cerebellum (Fig. 8E) than control mice. The infiltration of $CD4^+$ T cells was also observed in brains (Fig. 8F). In comparison with the wide distribution of $CD8^+$ T cells, $CD4^+$ T cells were relatively sparse and mainly distributed in some superficial layers of cerebral cortex and some perivascular regions (Fig. 8F), and $Axl^{-/-}$ mice showed greater number of $CD4^+$ T cells in cerebral cortex (Fig. 8G) and perivascular region (Fig. 8H) than control mice. We also detected the infiltration of T lymphocytes by using flow cytometry and found that consistent with the IHC results, $Axl^{-/-}$ mice displayed larger number of $CD8^+$ T cells and $CD4^+$ T cells in both cerebral cortex and hippocampus (Fig. 9A and 9B). The above data suggest that Axl deficiency enhances T lymphocytes infiltration in brain, which may promote brain damage during JE.

Axl Deficiency Boosts Pro-Inflammatory Cytokines Production in Brain

We next measured a panel of cytokines (IL-1α, IL-1β, IL-2, IL-4, IL-6, IL-10, TNF-α, IFN-γ, CCL2, and CCL5) in brain at 7 dpi, which mediate inflammatory response. Under mock treatment, $Axl^{-/-}$ mice showed similar baseline levels of all the assayed cytokines with control mice (Fig. 10, mock). After infection, IL-2, IL-6, IFN-γ, CCL2, and CCL5 significantly elevated in brain, and $Axl^{-/-}$ mice showed much higher levels of these cytokines

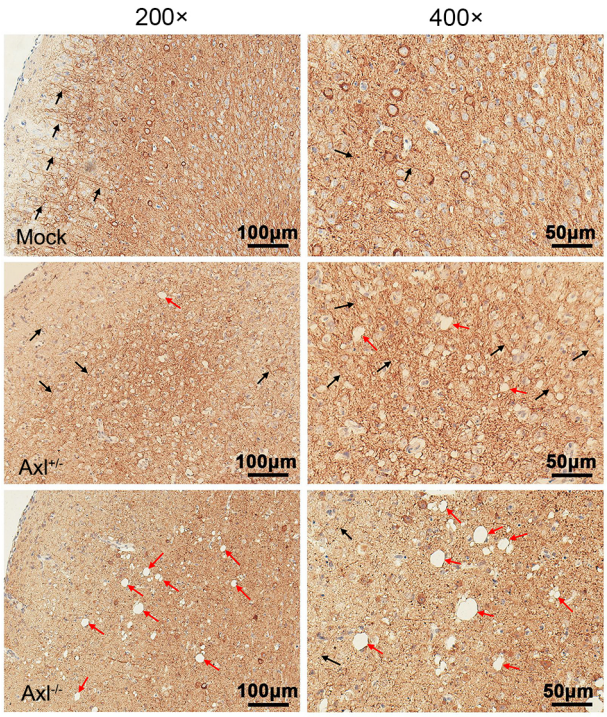

Fig. 6 Immunohistochemical staining of neurofilament. Four-week-old $Axl^{+/-}$ and $Axl^{-/-}$ mice were intraperitoneally injected with 10^4 PFU of JEV (infected) or PBS (mock). Brains were collected at 7 dpi and sagittally sectioned into 5 μm slides. SMI32 was used to visualize neurofilaments in cerebral cortex. Black arrows denote neurofilaments; red arrows denote neuron death. This image is the representative of four $Axl^{+/-}$ and four $Axl^{-/-}$ mice.

than control mice (Fig. 10, infected). These results suggest that Axl deficiency aggravates the production of pro-inflammatory cytokines in brain after JEV infection. These pro-inflammatory cytokines may work together with the infiltrated inflammatory cells to enhance neuroinflammation and deteriorate brain damage.

Discussion

JEV infection in brain causes a severe encephalitis called JE, which threatens people's health in 24 countries and is the most commonly diagnosed viral encephalitis in the world. Unfortunately, we have very limited countermeasures to specifically therapy JE, which is due to insufficient knowledge about JEV and JE pathogenesis. Axl has been reported to alleviate inflammatory damage through inhibiting production of a range of pro-inflammatory cytokines. However, its role in encephalitis has been less studied, let alone viral encephalitis. We have previously reported that during JEV infection, Axl deficient mice manifested more severe body weight loss than control mice, which we think is probably due to the loss of anti-inflammatory effect of Axl. In this study, by using $Axl^{-/-}$ and control mice, we assessed the role of Axl in JE pathogenesis. We found Axl deficiency accelerated JE progression, which is associated with exacerbated brain lesions, characterized with increased neuron apoptosis, extended inflammatory cells infiltration, and enhanced

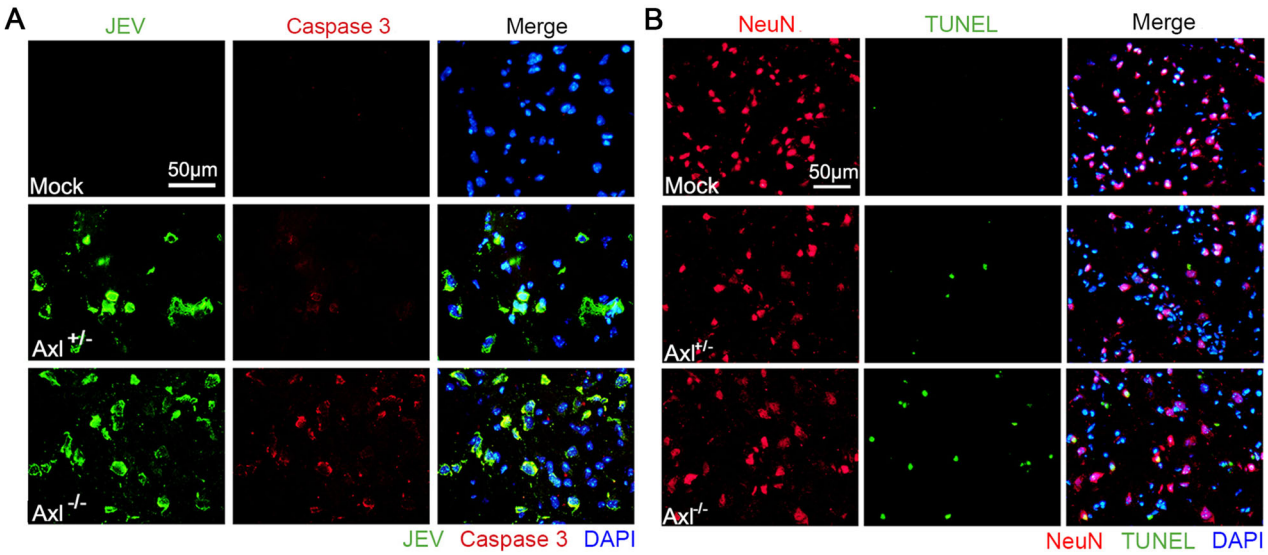

Fig. 7 The effect of Axl on the apoptosis of JEV-infected neurons. Four-week-old $Axl^{+/-}$ and $Axl^{-/-}$ mice were intraperitoneally injected with 10^4 PFU of JEV (infected) or PBS (mock). Brains were collected at 7 dpi and sectioned into 6 μm slides. **A** Immunofluorescent co-staining of JEV antigens and cleaved caspase 3, scale bar = 50 μm. **B** Immunofluorescent co-staining of NeuN and TUNEL (a marker for damaged DNA), scale bar = 50 μm. This image is the representative of four $Axl^{+/-}$ and four $Axl^{-/-}$ mice.

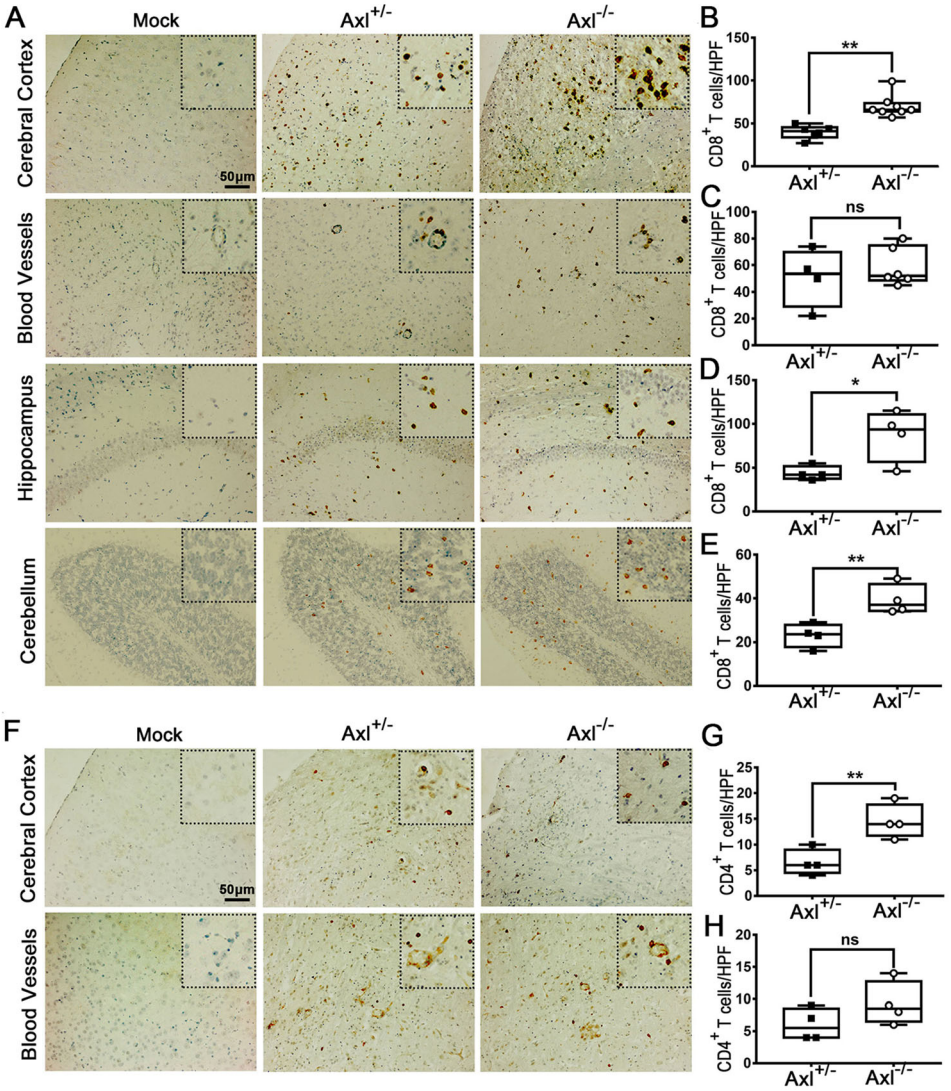

Fig. 8 T lymphocytes infiltration in brain during JE. Four-week-old $Axl^{+/-}$ and $Axl^{-/-}$ mice were intraperitoneally injected with 10^4 PFU of JEV (infected) or PBS (mock). Brains were collected at 7 dpi and sectioned into 5 μm slides. $CD8^+$ T cells and $CD4^+$ T cells were demonstrated by IHC staining. **A** Representative IHC image depicting $CD8^+$ T cell infiltration in brain at 7 dpi of JE present mice, scale bar = 50 μm. **B–E** Quantitative analysis of the number of $CD8^+$ T cells per high power field (HPF) in cerebral cortex (**B**), perivascular region (**C**), hippocampus (**D**), and cerebellum (**E**). **F** Representative IHC image depicting $CD4^+$ T cell infiltration in brain at 7 dpi of JE present mice, scale bar = 50 μm. **G, H** Quantitative analysis of the number of $CD4^+$ T cells per HPF in cerebral cortex (**G**) and perivascular region (**H**). Data were expressed as the median + upper and lower quartiles, and each dot represents a mouse, $^*P < 0.05$, $^{**}P < 0.01$, and ns $P > 0.05$, as analyzed by Mann–Whitney test.

production of pro-inflammatory cytokines. Our results thus reveal an anti-inflammatory and neuroprotective role of Axl in JE and suggest Axl may be a therapeutic target for JE.

Axl is a key member of TAM family, which has been reported to attenuate production of pro-inflammatory cytokines in multitudinous cells and tissues (Rothlin *et al.* 2007; Siemann *et al.* 2017). Activation of Axl signaling mitigates lung edema and alveolar inflammation in acute lung injury induced by ischemia–reperfusion by inhibiting production of pro-inflammatory cytokines including IL-1β, IL-6, and TNF-α (Peng *et al.* 2019). In a mouse model of autoimmune thyroiditis, stimulation of Axl signaling by Gas6 significantly reduces the incidence of thyroiditis, the infiltration of lymphocytes, and the production of pro-inflammatory cytokines (Sun *et al.* 2019). Axl also reduces severity of arthritis in a mouse model of arthritis (Waterborg *et al.* 2019). However, in some diseases, Axl plays contradictory role in regulating production of pro-inflammatory cytokines and chemokines. In a mouse model of glomerulonephritis, knockout or inhibition of Axl significantly reduces production of renal inflammatory cytokine and chemokine and improved kidney function (Zhen *et al.* 2018). Axl activation by Gas6 in pregnant rats significantly increases level of diverse pro-inflammatory cytokines in sera such as TNF-α, IFN-γ, IL-1α, IL-1β, and IL-6, and also increases placenta oxidative stress and apoptosis (Hirschi *et al.* 2019). Both Axl and its ligand Gas6 are abundantly expressed in the central nervous system, suggesting that Axl may have important function in brain (Shafit-Zagardo *et al.* 2018). However, up to now, the studies pertaining to the roles of Axl in encephalitis are very few, let alone viral encephalitis. Activation of Axl signaling alleviates neuroinflammation and neurological deficits after ischemic stroke (Wu *et al.* 2018). Axl knockout causes extensive axonal damage, prolonged neuroinflammation, and less remyelination after cuprizone induced encephalitis (Ray *et al.* 2017). Axl knockout leads

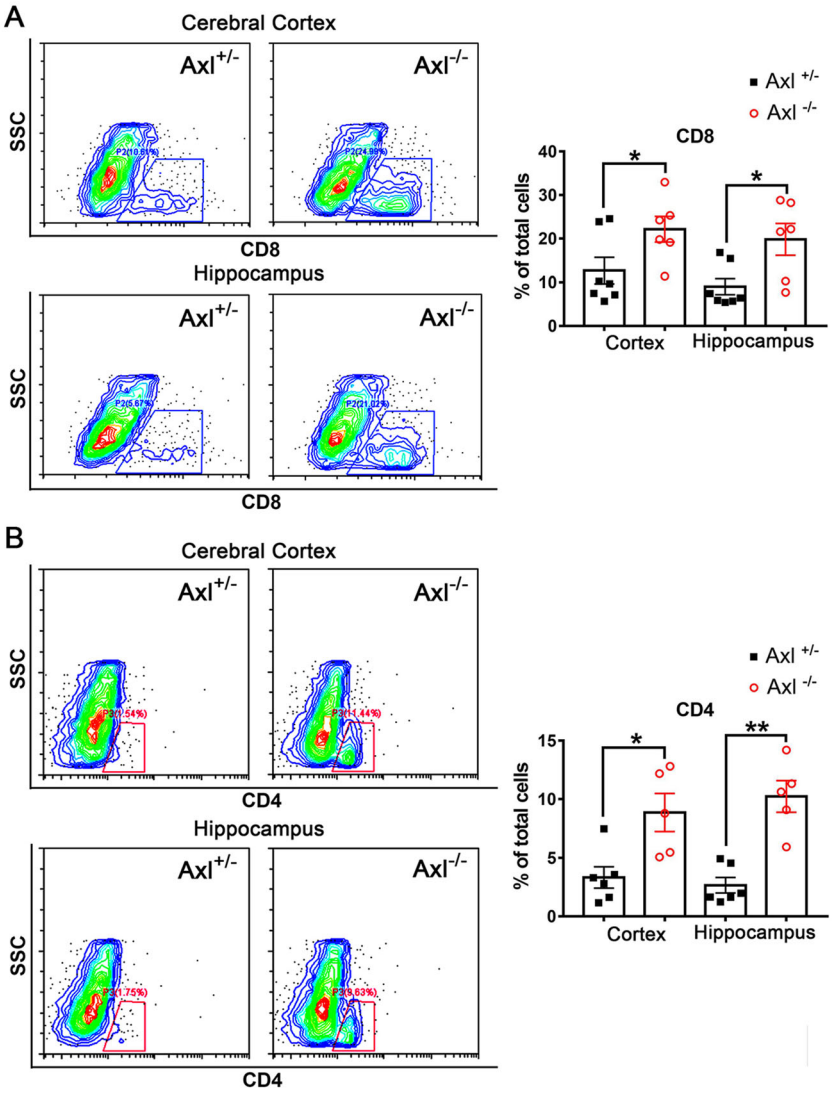

Fig. 9 Detection of T lymphocytes in brain by flow cytometry. Percentage of $CD8^+$ T cells (**A**) and $CD4^+$ T cells (**B**) in cerebral cortex and hippocampus at 7 dpi. Each dot denotes a mouse, $*P < 0.05$, $**P < 0.01$, as analyzed by Student's t test.

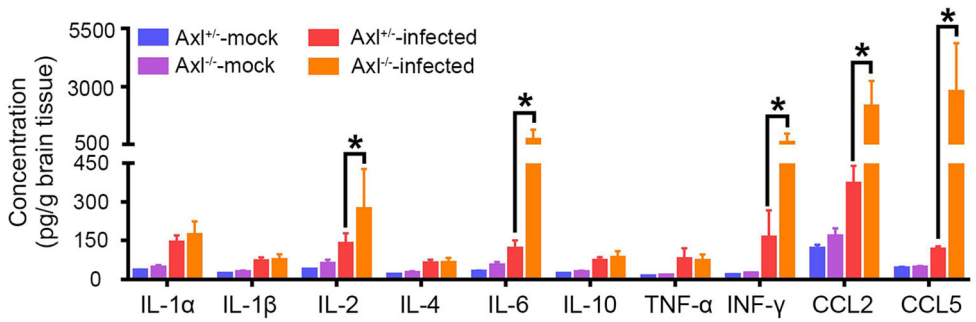

Fig. 10 Inflammatory cytokines measurement in brain. Four-week-old $Axl^{+/-}$ and $Axl^{-/-}$ mice were i.p. injected with 10^4 PFU of JEV (infected) or PBS (mock). Brains were collected at 7 dpi and subjected to Aimplex immunoassay for cytokines measurement. Data are expressed as the mean ± SEM, n = 6 for each group, $*P < 0.05$, as analyzed by Student's t test.

to enhanced inflammation in the CNS and delayed removal of myelin debris during experimental autoimmune encephalomyelitis (Weinger *et al.* 2011). TAM triple knockout mice exhibit systemic autoimmune diseases, characterized by increased pro-inflammatory cytokine production, autoantibody deposition and autoreactive lymphocyte infiltration into brain (Li *et al.* 2013). In our own results, Axl deficiency increases neuron apoptosis and

axonal damage, promotes production of several pro-inflammatory cytokines and chemokines, and facilitates infiltration of cytotoxic immunocytes, suggesting that Axl is an anti-inflammatory and neuroprotective factor during JE.

The molecular mechanism by which Axl regulates the inflammatory response in brain remains unclear and needs to be further studied. Notwithstanding, some investigations prove that activation of Axl signaling can inhibit Toll like receptors (TLRs) and TLRs-mediated cytokines production in human astrocytes, human glial cells, and human Sertoli cells via upregulating SOCS1 and SOCS3 (Rothlin *et al.* 2007; Meertens *et al.* 2017; Chen *et al.* 2018; Strange *et al.* 2019). This mechanism has been demonstrated to exist universally in various cell types, which may shed light on the understanding of the mechanism underlying Axl's anti-inflammation function during JE.

In summary, our work revealed that Axl alleviates brain damage and delays encephalitis progression by inhibiting the generation of pro-inflammatory cytokines, impeding the infiltration of cytotoxic immune cells, and promoting the survival of neural cells. These results suggest that Axl is a neuroprotective factor against JE pathogenesis and it may act as a potential target for alleviating inflammatory damage of JE.

Acknowledgements This work was supported by the National Natural Science Foundation of China (81671971, 81871641, 81972979, U1902210 and U1602223), the Scientific Research Plan of the Beijing Municipal Education Committee (KM201710025002), and the Key Project of Beijing Natural Science Foundation B (KZ201810025035), the Support Project of High-level Teachers in Beijing Municipal Universities in the Period of 13th Five-year Plan (IDHT20190510).

Author contributions ZY Wang designed and performed most of the experiments, analyzed the data, wrote and reviewed the manuscript. ZD Zhen performed flow cytometry experiments and TUNEL staining. DY Fan maintained cells, viruses, and reagents. PG Wang and J An conceived the project, analyzed the data, and finalized the manuscript.

Compliance with Ethical Standards

Conflict of interest The authors declare that they have no conflict of interest.

Animal and Human Rights Statement All institutional and national guidelines for the care and use of laboratory animals were followed, and all the animal experiments were approved by the Experimental Animal Welfare and Animal Ethics Committee of Capital Medical University, Beijing, China (permission code: AEEI-2015–048; permission date: April 20, 2015).

References

Amicizia D, Zangrillo F, Lai PL, Iovine M, Panatto D (2018) Overview of Japanese encephalitis disease and its prevention. Focus on IC51 vaccine (IXIARO ®). J Prev Med Hyg 59:E99–E107

Chen J, Yang YF, Yang Y, Zou P, He Y, Shui SL, Cui YR, Bai R, Liang YJ, Hu Y, Jiang B, Lu L, Zhang X, Liu J, Xu J (2018) AXL promotes Zika virus infection in astrocytes by antagonizing type I interferon signalling. Nat Microbiol 3:302–309

Hirschi KM, Tsai KYF, Davis T, Clark JC, Knowlton MN, Bikman BT, Reynolds PR, Arroyo JA (2019) Growth arrest specific protein (Gas)-6/AXL signaling induces preeclampsia (PE) in rats. Biol Reprod. https://doi.org/10.1093/biolre/ioz140

Li Q, Lu Q, Lu H, Tian S (2013) Systemic autoimmunity in TAM triple knockout mice causes inflammatory brain damage and cell death. PLoS ONE 8:e64812

Meertens L, Labeau A, Dejarnac O, Cipriani S, Sinigaglia L, Bonnet-Madin L, Le Charpentier T, Hafirassou ML, Zamborlini A, Cao-Lormeau VM, Coulpier M, Misse D, Jouvenet N, Tabibiazar R, Gressens P, Schwartz O, Amara A (2017) Axl mediates ZIKA virus entry in human glial cells and modulates innate immune responses. Cell Rep 18:324–333

Moller-Tank S, Maury W (2014) Phosphatidylserine receptors: enhancers of enveloped virus entry and infection. Virology 468–470:565–580

Peng CK, Wu CP, Lin JY, Peng SC, Lee CH, Huang KL, Shen CH (2019) Gas6/Axl signaling attenuates alveolar inflammation in ischemia-reperfusion-induced acute lung injury by up-regulating SOCS3-mediated pathway. PLoS ONE 14:e0219788

Ray AK, DuBois JC, Gruber RC, Guzik HM, Gulinello ME, Perumal G, Raine C, Kozakiewicz L, Williamson J, Shafit-Zagardo B (2017) Loss of Gas6 and Axl signaling results in extensive axonal damage, motor deficits, prolonged neuroinflammation, and less remyelination following cuprizone exposure. Glia 65:2051–2069

Richard AS, Shim BS, Kwon YC, Zhang R, Otsuka Y, Schmitt K, Berri F, Diamond MS, Choe H (2017) AXL-dependent infection of human fetal endothelial cells distinguishes Zika virus from other pathogenic flaviviruses. Proc Natl Acad Sci U S A 114:2024–2029

Rothlin CV, Carrera-Silva EA, Bosurgi L, Ghosh S (2015) TAM receptor signaling in immune homeostasis. Annu Rev Immunol 33:355–391

Rothlin CV, Ghosh S, Zuniga EI, Oldstone MB, Lemke G (2007) TAM receptors are pleiotropic inhibitors of the innate immune response. Cell 131:1124–1136

Seitz HM, Camenisch TD, Lemke G, Earp HS, Matsushima GK (2007) Macrophages and dendritic cells use different Axl/Mertk/Tyro3 receptors in clearance of apoptotic cells. J Immunol 178:5635–5642

Shafit-Zagardo B, Gruber RC, DuBois JC (2018) The role of TAM family receptors and ligands in the nervous system: from development to pathobiology. Pharmacol Ther 188:97–117

Sheng Z, Gao N, Cui X, Fan D, Chen H, Wu N, Wei J, An J (2016) Electroporation enhances protective immune response of a DNA vaccine against Japanese encephalitis in mice and pigs. Vaccine 34:5751–5757

Siemann DN, Strange DP, Maharaj PN, Shi PY, Verma S (2017) Zika virus infects human sertoli cells and modulates the integrity of the in vitro blood-testis barrier model. J Virol 91

Strange DP, Jiyarom B, Pourhabibi Zarandi N, Xie X, Baker C, Sadri-Ardekani H, Shi PY, Verma S (2019) Axl Promotes Zika Virus Entry and Modulates the Antiviral State of Human Sertoli Cells. mBio 10

Sun B, Qi N, Shang T, Wu H, Deng T, Han D (2010) Sertoli cell-initiated testicular innate immune response through toll-like receptor-3 activation is negatively regulated by Tyro3, Axl, and mer receptors. Endocrinology 151:2886–2897

Sun X, Guan H, Peng S, Zhao Y, Zhang L, Wang X, Li C, Shan Z, Teng W (2019) Growth arrest-specific protein 6 (Gas6) attenuates inflammatory injury and apoptosis in iodine-induced NOD.H-2(h4) mice. Int Immunopharmacol 73:333–342

Turtle L, Solomon T (2018) Japanese encephalitis - the prospects for new treatments. Nat Rev Neurol 14:298–313

Wang R, Liao X, Fan D, Wang L, Song J, Feng K, Li M, Wang P, Chen H, An J (2018) Maternal immunization with a DNA vaccine candidate elicits specific passive protection against postnatal Zika virus infection in immunocompetent BALB/c mice. Vaccine 36:3522–3532

Waterborg CEJ, Broeren MGA, Blaney Davidson EN, Koenders MI, van Lent P, van den Berg WB, van der Kraan PM, van de Loo FAJ (2019) The level of synovial AXL expression determines the outcome of inflammatory arthritis, possibly depending on the upstream role of TGF-beta1. Rheumatology (Oxford) 58:536–546

Weinger JG, Brosnan CF, Loudig O, Goldberg MF, Macian F, Arnett HA, Prieto AL, Tsiperson V, Shafit-Zagardo B (2011) Loss of the receptor tyrosine kinase Axl leads to enhanced inflammation in the CNS and delayed removal of myelin debris during experimental autoimmune encephalomyelitis. J Neuroinflammation 8:49

Wu G, McBride DW, Zhang JH (2018) Axl activation attenuates neuroinflammation by inhibiting the TLR/TRAF/NF-kappaB pathway after MCAO in rats. Neurobiol Dis 110:59–67

Yuan A, Rao MV, Veeranna, Nixon RA (2017) Neurofilaments and Neurofilament proteins in health and disease. Cold Spring Harb Perspect Biol 9:a018309

Zhen Y, Lee IJ, Finkelman FD, Shao WH (2018) Targeted inhibition of Axl receptor tyrosine kinase ameliorates anti-GBM-induced lupus-like nephritis. J Autoimmun 93:37–44